The Spatiality of Swarms —
Quantitative Analysis of Dynamic Interaction Networks

Sebastian von Mammen and Christian Jacob

University of Calgary, Alberta, Canada
{s.vonmammen,cjacob}@uclagary.ca

Abstract

Many mathematical models, which try to capture emergent phenomena, are based on state transitions that depend on neighborhood relationships. Cellular Automata (CA) and Random Boolean Networks (RBN) are examples of such models, where connectivity patterns determine the flow of signals among interconnected units. Whereas neighborhoods in CA and RBNs remain static, the focus of our investigations are artificial swarms that act in three-dimensional space, where neighborhood relationships among the swarming agents change over time. In fact, it is through the dynamically changing neighbors that determine a swarm system's overall behavior. In this paper we explore neighborhood dynamics of swarms and ask the question how each agents' time-dependent perception of its neighbors relates to specific flocking formations. We give examples of 'neighborhood functions' for choreographed swarming behaviors, such as line and figure-eight formations. We also evolve control parameters for swarm agents such that they approximate specific neighborhood functions that trigger switching and oscillations.

Introduction

Complex systems in nature usually comprise large numbers of interacting units, as for instance immune system cells that swarm in our bodies to fight off pathogens and remove damaged cells (Litman et al. (2005)). However, it already takes great effort to create and analyze stochastic models of only a few interacting units (Oilek and Klein (1979)).

Numerical experiments have been playing an increasingly important role in the investigation of complex systems (Neelamkavil (1994)). In order to build numerical models of complex systems, it is necessary to identify those features of natural systems that are crucial for the emergence of the phenomena of interest (Dasgupta (2006)). In particular, complex patterns that appear in natural systems, form in space and unfold over time, have been reproduced in models built from large sets of computational units that change their states in accordance with their local neighborhoods. Cellular Automata (Wolfram (1984)) and Random Boolean Networks (Kauffman (1995)) are examples of such models, both of which will be outlined in the subsequent section on related work.

Like in natural swarms — such as bird flocks or fish schools —, the neighborhoods of artificial swarm individuals change constantly and depend on preceding interactions. Therefore, artificial swarms represent a model of complex phenomena that embraces dynamical neighborhood relationships. We explain this idea in detail in the third section.

In order to capture the formation of neighborhood relations in swarms, we measure the numbers of neighbors for every individual at each simulated time step, within a particular neighborhood radius. We show examples of neighborhood evolutions and discuss these through swarms that exhibit specific flocking formations.

Subsequently, we demonstrate that switching and oscillating neighborhood formations can be achieved in homogeneous swarm systems whose flight is solely regulated by a linearly scaled acceleration of the individuals. We conclude this paper with a summary and an outlook on future work.

Related Work

In *Cellular Automata* (CA) the processing units (*cells*) are organized in a lattice structure and are set to an initial state that is changed in accordance with a set of rules that consider the states of all neighboring cells. CAs were primarily developed to model phenomena of self-reproduction based on the interplay among a large number of finite state machines (von Neumann and Burks (1966)). Not only was this goal finally achieved (Gardner (1970)), but CA also became a general model for complex systems based on neighborhood-dependent state changes (Wolfram (2002)). According to Wolfram (1984), patterns emerging from binary cellular automata can be classified into four different categories:

1. spatially homogeneous state;
2. sequence of simple stable or periodic structures;
3. chaotic aperiodic behaviour;
4. complicated localized structures, some propagating.

The transition from one such class or phase to another is of considerable interest for various models of natural phenomena such as the spreading of infectious diseases (del Rey

et al. (2006)). We will explore similar transitions for swarming agents in 3D space, for which their neighbors change dynamically over time.

Whereas in CA cells have a fixed spatial arrangement, *Random Boolean Networks* or 'RBNs' (Kauffman (1995)) abstract from the notion of space. Here, each cell can be connected to any other one, forming an information propagating network. As in CAs, the configuration of all cells defines the global system state.

Albert et al. conducted experiments to create and analyze random RBN with the same distributions of degrees of connectivity as those shown in gene regulatory networks (Albert (2004)), and other scale-free networks (Hidalgo and Barabasi (2006)). It has been demonstrated that RBN models show state transition patterns very similar to those of natural networks (Serra et al. (2003)).

Swarms as a Model of Complexity

Once determined, the neighborhood relations between the units of a CA or RBN remain fixed. One may assume, however, that in many natural phenomena different forces draw and push the involved units so that they change their positions, as is observed in bird flocks, fish schools, ant colonies, cell development. Thereby, of course, the neighborhoods of the units do not remain static.

Exactly this idea is captured in the 'swarm metaphor'. Large sets of swarm individuals, or agents, attract and repel each other. The neighborly influence felt by one individual determines its action for the next time step. A swarm agent changes its velocity and position, thereby gaining a new neighborhood perspective and, at the same time, altering its neighbors' perspectives. Consequently, a feedback loop of actions and reactions emerges. Unlike in CA and RBN, state changes directly impact neighborhood bonds. We argue that this feedback loop between agents and their changing neighbor arrangements is the key feature to model spatially organized systems, since locality plays a crucial role for any effective interaction.

Reynolds (1987) presented a computational model to simulate flocking formations as seen in birds or herds of animals. Here, a set of agents, called *boids*, perceive and react to each other in three-dimensional space. A formal description of Reynolds' flocking model was provided by Kwong and Jacob (2003) who interactively evolved different flight formations of boids. In particular, a boid perceives its neighbors within a viewing cone of length l and angle α (Figure 1). A boid reacts to its n neighbors by an alignment urge $\vec{v}_a$, by attraction towards and repulsion from the geometric center of the neighbors $\vec{v}_c$, and, if they get too close, by a separation urge $\vec{v}_s$. Fluctuations are introduced into the flight pattern by adding a weighted random unit-vector $\vec{v}_r$ to the acceleration. A boid's velocity and acceleration are limited by two values: v_{max} and a_{max}, respectively. Additionally, a world center $\vec{w}$ is provided that determines the swarm's
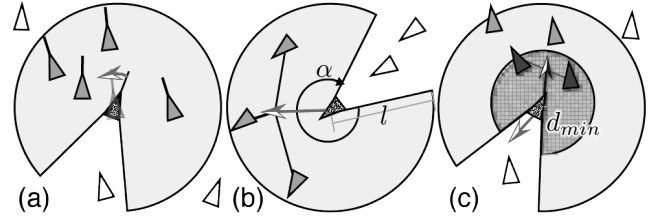

Figure 1: The three basic flocking urges alignment (a), cohesion (b) and separation (c) are depicted as they would influence (grey arrows with b/w head) the central agents (pixelized). White agents are out of scope, grey ones are within the neighborhood vicinity and dark grey ones are close enough to trigger separation. The diagrams are adapted from Craig Reynolds' website *http://www.red3d.com/cwr/boids/*.

flight destination. In order to compute boid i's acceleration $\vec{a}_i$ and resulting velocity $\vec{v}_i$ and position $\vec{p}_i$ one has to determine its set of neighbors, N_i. All those agents in $S_i \subseteq N_i$ whose distance to i is smaller than d_{min} assume a special role by contributing to i's separation urge. Once its set of neighbors is determined, the acceleration vector of a boid results from the following weighted sum of urges.

$$\vec{a}_i = c_a \vec{v}_a + c_c \vec{v}_c + c_s \vec{v}_s + c_w \vec{v}_w + c_r \vec{v}_r \quad (1)$$

$$\vec{v}_a = \frac{1}{|N_i|} \sum_{j \in N_i} \vec{v}_j \quad (2)$$

$$\vec{v}_c = \frac{1}{|N_i|} \sum_{j \in N_i} \vec{p}_j \quad (3)$$

$$\vec{v}_s = \frac{1}{|S_i|} \sum_{j \in S_i} \vec{p}_j \quad (4)$$

$$\vec{v}_w = \vec{w} - \vec{p}_i \quad (5)$$

Neighborhood relations depend on the sight, the orientation and the position of the seeing individual, on the position of the potentially perceived individual, as well as on time.[1]

We want to point out that the emerging causal chain of boid interactions can be expressed as follows (Figure 2): The actions of a swarm agent i change its state which influences all those agents that are seeing i. At the same time i's new state results in the perception of a certain set of neighbors. These neighbors influence i's actions and the feedback loop starts all over again.

It is worthwhile noting that the system state and the neighborhood configuration are inseparable in the outlined swarm model. As a consequence, the observation of alterations of neighborhoods can be utilized to describe the system dynamics. Therefore, we measure the numbers of perceived neighbors $n(t) = |N_i(t)|$ of each swarm agent i at any given

---

[1] All vectors $\vec{a}_i$, $\vec{v}_a$, $\vec{v}_c$, $\vec{v}_s$, $\vec{v}_w$ and sets S_i and N_i are time-dependent, but we will not denote the time variable explicitly.
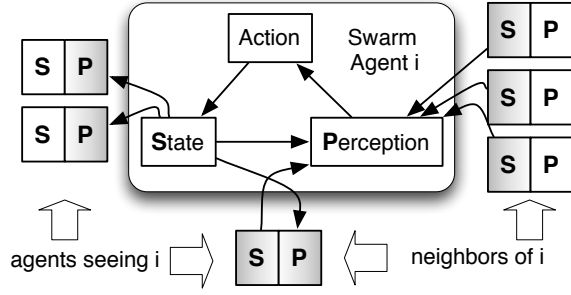
Figure 2: The slim arrows in the upper box show the direction of influence between perception, action and state of a swarm agent i. The S-P tuples stand for the state and perception modules of other agents that interact with i.

point in time t. We characterize a single state of the whole swarm by the average neighbor value of all M swarm individuals. That is, we define the time-dependent neighborhood function for a swarm with M agents as

$$\bar{n}(t) = \frac{1}{M} \sum_{i=0}^{N} n_i(t). \qquad (6)$$

Finally, we suggest the evolution of $\bar{n}(t)$ over the course of time to analyze and describe the dynamics of the (swarm) system. Based on this approach we investigate various flocking formations of boid swarms in the next section.

Analysis of Flock Formations

Kwong and Jacob (2003) have shown that diverse flocking behaviors of boids can be evolved with different parameter sets for Equations 1 to 5. We utilize four sets of flocking parameters from this work (Table 1) to analyze 'choreographic' line formations and figure-eight formations based on $\bar{n}(t)$. Two different swarm configurations are provided for each formation type. The following analysis links several phases of swarm interactions and the occurrences of desired formations to the development of the neighborhood function $\bar{n}(t)$. The presented results are all produced by 50 swarm agents with a perception radius $l = 3.5$ and viewing angle $\alpha = 2.0$. As above, we normalize all $\bar{n}(t)$ values by the number of active swarm agents.

Line Formations

Figure 3 shows the development of $\bar{n}(t)$ with the line formation parameters in row (i) of Table 1. The graph shows the average number of neighbors perceived by each agent over time. The plot can be partitioned into five distinct phases. In phase I, the average neighborhood perception $\bar{n}$ is rising rapidly. Mainly the urge towards the world center $\vec{w} = (0,0,0)^T$ accelerates the initially stationary agents towards each other (Figure 4 (a) to (c)), ending up much closer

than before (Figure 4 (d)). In fact, this phase was already described by Reynolds (1987).

Line formations

	c_a	c_c	c_s	c_w	c_r	a_{max}	v_{max}	d_{min}
(i)	7	8	5	5	5	38	13	0.14
(ii)	7	8	4	10	4	40	9	0.01

Figure-eight formations

	c_a	c_c	c_s	c_w	c_r	a_{max}	v_{max}	d_{min}
(i)	3	10	1	5	2	38	6	0.01
(ii)	5	10	2	12	1	35	6	0.34

Table 1: Evolved parameter sets for 'choreographically' flocking swarms (Kwong and Jacob (2003)).
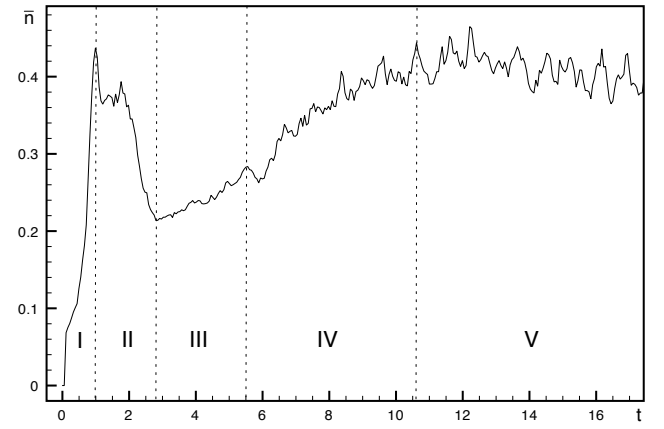

Figure 3: Developments of the average neighborhood perception $\bar{n}(t)$ matches several phases of agent interactions and flock formations.
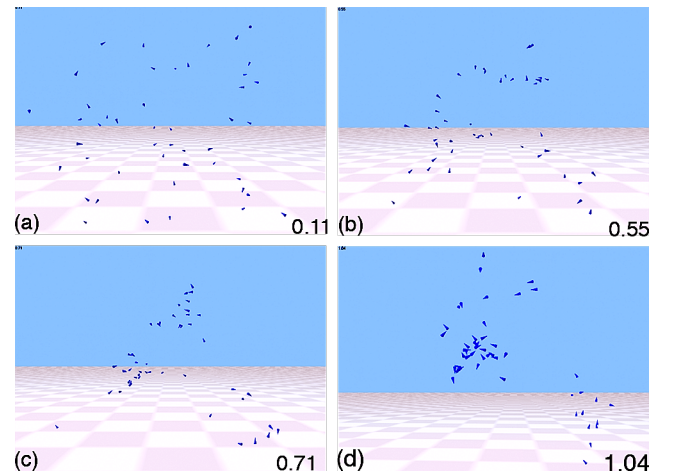

Figure 4: In phase I initially stationary agents are drawn together by the urge towards the world center.

During cluster formation the agents gain momentum by-passing many other agents. This leads to the decreasing average neighborhood perception in Phase II. As a result, several smaller flocks emerge after these two initial phases (Figure 5). The cohesion urge is now strong enough to keep subgroups of agents together that gather in the same vicinities (Figure 5 (a)). The alignment urge transforms these subgroups into flocks that exhibit increasingly homogeneous flight patterns (Figure 5 (b)).
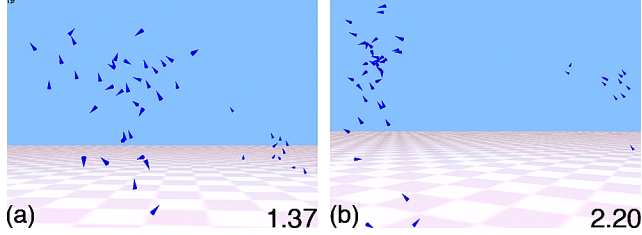

(a) 1.37 (b) 2.20

Figure 5: In phase II subgroups align as separate flock formations.

In phase III of Figure 3, a line formation emerges (Figure 6 (a)), yielding relatively small values of $\bar{n}$. Steadily, the agents are drawn closer to each other and $\bar{n}(t)$ increases accordingly. In phase IV a dense agglomeration of agents emerges at the head of the line formation (Figure 6 (b)). Eventually, the line formation is destroyed and substituted by a tight cluster formation (Figure 6(c)). After reaching phase V, the flock remains in a quasi steady state that is subject to only minor fluctuations (Figure 6(d)).

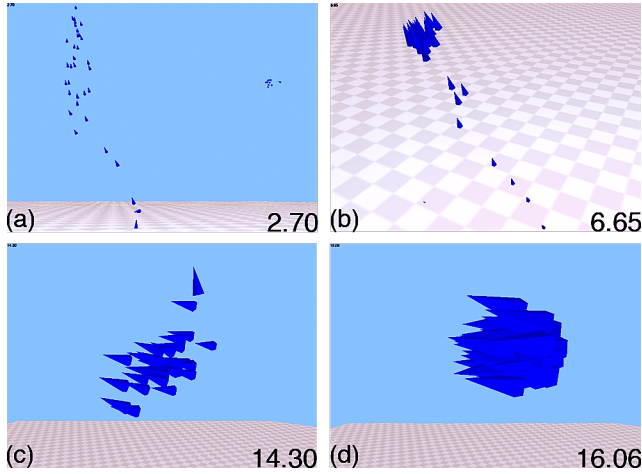(a) 2.70 (b) 6.65

(c) 14.30 (d) 16.06

Figure 6: (a) Phase III: agents of single flocks follow each other in a line formation. (b) Phase IV: agents gather into dense clusters at the heads of the line formations. (c) and (d) Phase V: a tight cluster has formed that is robust enough against sporadic attempts of separation.

Changing the simulation to the line formation (ii) pa-

rameters in Table 1 results in increased randomness of the agents' acceleration. The swarm looses its tight, cohesive constraints and thereby allows for the sporadic escape of agents. Figure 7 shows the corresponding neighborhood function. The neighbors of a fleeing agent may try to catch up and break out of the cluster as well. Consequently, the swarm's flight is dominated by tight cluster formations but is frequently interrupted by line formations (Figure 8). Another consequence is that single agents or even whole flocks can leave the parent flock, so that eventually all agents are dispersed and unable to interact.
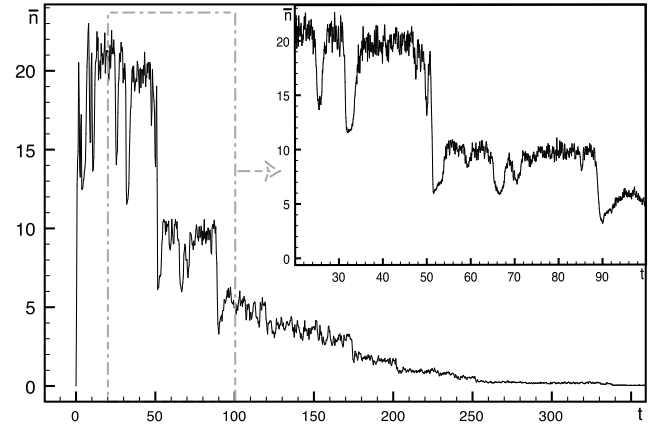

Figure 7: In the simulation of line formation (ii) of Table 1 agents break out of tightly formed clusters and take the lead of long line formations. During such events $\bar{n}$ drops temporarily (e.g. at $t = 25$ and $t = 32$). Frequently the line formations break up (as in Figure 6) and the parting flocks do not interact anymore ($t = 50$). As a consequence, $\bar{n}(t)$ reaches a value of zero at about $t = 400$.

(a) 50.76 (b) 51.26
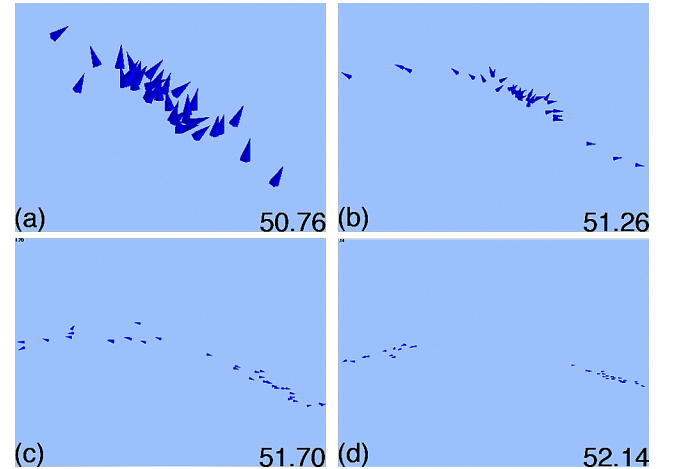
(c) 51.70 (d) 52.14

Figure 8: An agent cluster is breaking up into two line formations, one urging upwards, one towards the floor.

Figure-Eight Formations

In analogy to the discussed line formation examples, we investigate two boid configurations that exhibit figure-eight flight patterns with respect to $\bar{n}(t)$. As we can see in Figure 9, parameter configuration (i) from Table 1 reaches a steady state, whereas with setting (ii) agents repeatedly wander through different phases to eventually spread all agents far enough from each other to prevent further interaction — exactly as in line formation (ii) and in Figure 7.

Configuration (i) rapidly swings into a figure-eight formation traced by small clusters of six to ten agents (Figure 10 (b)). Here, the swarm constantly traverses through a limit cycle of global states as indicated by the fast oscillating values of $\bar{n}$ (Figure 9 (i)). In comparison to the line formation experiments, the oscillation of $\bar{n}$ is characteristic for figure-eight formations. Furthermore, for configuration (i) the oscillation reached at about $t = 20$ marks a quasi steady state.

In figure-eight configuration (ii) the neighborhood perception converges towards zero, and the subgroups of swarm agents may break away during intermediary line formations. This is similar to the second line formation experiment.

Line formations, such as illustrated in Figure 11(a) are reflected by the steep drops of $\bar{n}(t)$ in Figure 9(ii). In general, line formations fold back quickly into figure-eight formations, as is shown in Figure 11(b).

In contrast to the line experiments, the difference between a configuration that quickly results in a stable equilibrium and a swarm that exhibits long periods of drastic changes cannot be directly inferred from the according flocking parameters in Table 1. We assume that in complex figure-eight flight patterns it becomes more difficult to identify a parameter, such as the random weight c_r in Eq. 1, as crucial for spontaneous behaviors.
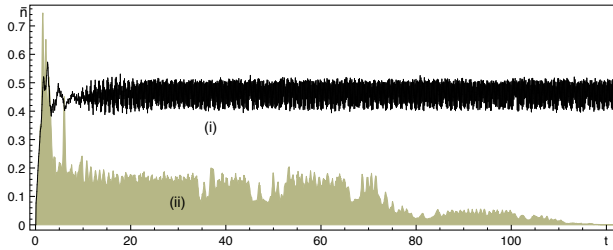

Figure 9: The development of $\bar{n}$ of figure-eight formations (i) and (ii) based on the parameter sets in Table 1.

Reverse Engineering of $\bar{n}(t)$

The examples in the previous section demonstrate how measuring the neighborhood dynamics over time can help to describe and analyze swarming behaviors. Now, we utilize this association to approximate neighborhood dynamics as
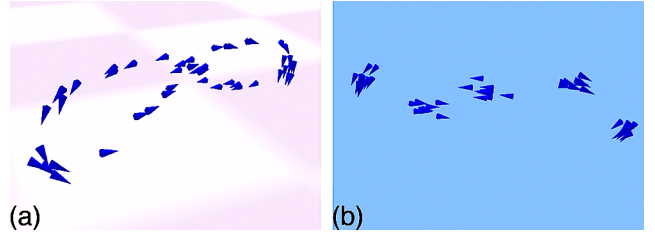

Figure 10: (a) Agents in figure-eight formation. (b) Tight agent flocks (of six to ten agents) in figure-eight formation.
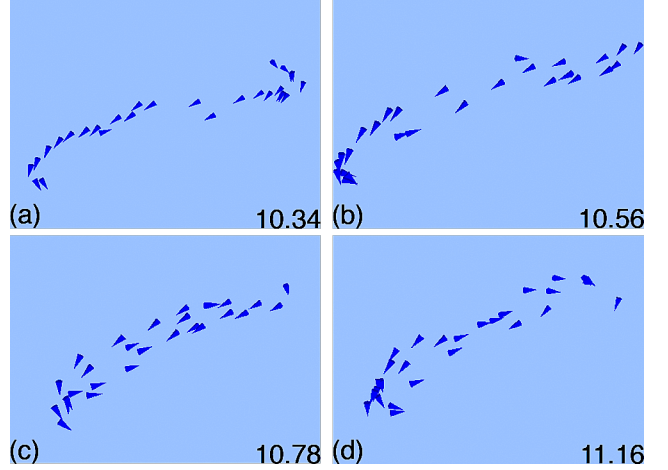

Figure 11: A line formation is about to collapse into a figure-eight pattern.

they might contribute to the coordination of naturally occurring phenomena, such as biological switches and clocks or timers.

The neighborhood value $n_i(t)$ of a single agent may change rapidly, remain fixed or oscillate. It is also easy to discover a whole flock of agents entering an equilibrium of a specific average neighbor value $\bar{n}(t)$. The results in the previous section also show that even a whole swarm can change dynamically, or, put differently, can follow specific evolutions of $\bar{n}(t)$.

If it was not for its contextual evolution, the average neighborhood $\bar{n}(t)$ would mainly characterize the concurrent spread, or density, of boid flocks, thereby corresponding much to the common view on molecular concentrations. In fact, neighborhood fluctuations indicate changes in the structure of swarms. Immediately, the question arises which patterns of movement could one expect when looking at evolutions of $\bar{n}(t)$ that correspond to the development of molecular concentrations in biological measurements.[2]

Even though the expression of genes happens stochas-

---

[2]Such measured molecular concentrations may come from microarray experiments that approximately capture the number of (reporter) proteins over time.

tically, the levels of expression can differ greatly which promotes the idea of a genetic switch (Jacob and Burleigh (2004)). By the approximation of a step function for $\bar{n}(t)$, we intend to show that even a homogeneous swarm could exhibit bi-stable switching behavior. Oscillations occur in natural systems as timers, such as circadian clocks. A a second option, we therefore explore which swarm behaviors can be evolved that follow a sinusoidal neighborhood function. For both endeavors we utilize a genetic algorithm that operates on populations of swarms as described in the following paragraphs.

Evolutionary Experiments

A homogeneous boid swarm, consisting of agents that share the same control parameters, are represented by a genotype vector $\vec{b} = (c_a, c_c, c_s, c_w, c_r, v_{max}, a_{max}, l, r)^T$. We also want to modify the starting positions, initial accelerations and initial velocities of the swarm agents: $init_0, init_1, ..., init_N$. The extended swarm genotype is therefore $\bar{g} = (\vec{b}, init_0, init_1, ..., init_N)$.

In the following experiments we provide a desired target function $x(t)$ for $\bar{n}$ and reward its approximation with a fitness value $f = 1/\left(\sum_{t=1}^{40} |\bar{n}(t) - x(t)|\right)$. We rely on the genetic operators of fitness proportionate selection, incremental mutation and multi-point crossover on all numeric values. A population counts 30 swarms, with each swarm consisting of 30 agents. The genetic algorithm was run up to 300 generations.

Step Function

As the computation of the genotype was limited to 40 simulated seconds, we decided to trigger the switch at about half of the overall time-frame. A difference of 0.5 units in a system with values $\bar{n} \in [0; 1)$ denotes an obvious leap, whereas $\bar{n} = 0.25$ is large enough to allow for further swarm interactions (as opposed to $\bar{n} = 0.0$ that rules out the possibility for local interactions).

$$x(t) = \begin{cases} 0.25 & t < 22 \\ 0.75 & t \geq 22 \end{cases}$$

Figure 12 displays the step function approximation of a boid configuration that appears after 200 generations of the outlined genetic algorithm. In Table 2 we list the parameters of the best evolved swarm genotype, which reveals two surprising values: $c_s = 1.0$ and $v_{max} = 0.0$. In fact, the velocity of the swarm individuals is greater than zero — the integration step of the simulation increases the velocity in accordance with the provided acceleration $\vec{a}$ that is limited to $a_{max} = 12.15$. The limitation of $v_{max} = 0.0$ means that the agent is stopped after each iteration, resulting in a very small velocity value, yet ensuring the orientation and alignment according to its flocking urges. As a consequence, starting from their initial positions, the agents are slowly converging

towards each other — nicely timed with the target function. The large weight for the separation urge $c_s = 1.0$ prevents the agents from getting too close and exceeding the target value of $x = 0.75$. The swarm is trained to approximate the step function for 40 simulated seconds. For that reason, the flight parameters are delicately balanced within this time frame. In the given example the swarm reaches an equilibrium shortly afterwards.
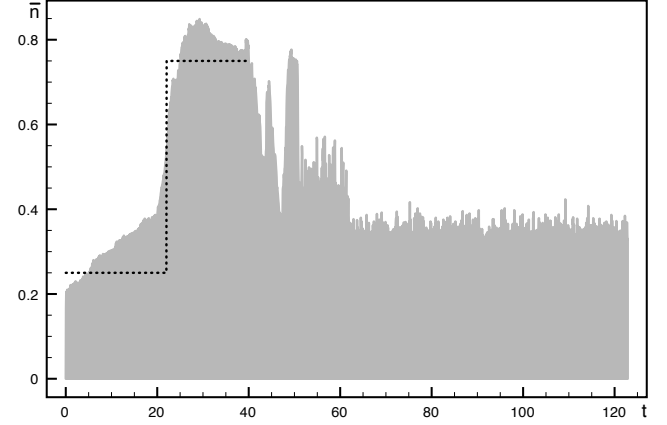

Figure 12: A neighborhood function $\bar{n}(t)$ of a boid configuration, bred by an evolutionary algorithm, approximates a step function as $\bar{x}(t)$. Afterwards, outside the evaluation window the swarm drops into an equilibrium with $\bar{n} \in [0.35; 0.45]$.

Boid configuration for $\bar{n}$ step function approximation

c_a	c_c	c_s	c_w	c_r	a_{max}	v_{max}	d_{min}
0.37	0.86	1.0	0.44	0.48	12.15	0.0	4.89

Table 2: Evolved swarm parameters that result in the neighborhood function of Figure 12, implementing a switch in $\bar{n}(t)$ ($\alpha = 2.09$, $l = 9.32$).

Sine Function

Two periods of a sine function are provided as target function $x(t)$ for time frame of 40 simulated seconds. As in the step function approximation, $\bar{n}$ is not forced to drop below 0.25 to guarantee a minimal space for interactions.

$$x(t) = sin(4\pi * t/40.0) * 0.25 + 0.5$$

Figure 13 shows the neighborhood function $\bar{n}(t)$ for the evolved swarm configuration as listed in Table 3. Eventually, at $t = 1244$ in Figure 14, the oscillation ends; this is when the agents form a tight cluster orbiting around the world center $\vec{w}$.

Since complex interactions render it difficult to identify certain flocking patterns, we activated motion blurring to

better capture the pattern formations of the swarm. We determined that the oscillation happens as the biggest flock repeatedly expands (Figure 15) and contracts (Figure 16). Leaps from a plateau to a local maximum, as seen at $t = 100$ in Figure 13, occur when formerly separated flocks rejoin (Figure 17). In Figure 18 several screenshots with activated motion blur illustrate intermediary flight formations.
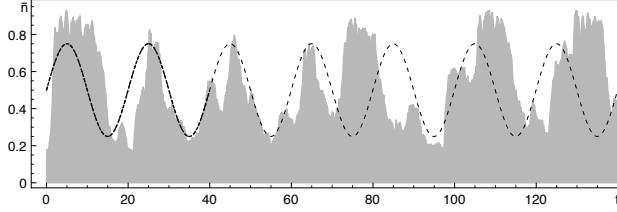

Figure 13: A boid configuration bred by an evolutionary algorithm approximates two periods of a sinusoidal neighborhood function. As shown, the oscillations sustain even afterwards.
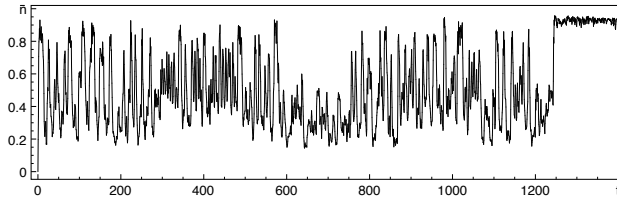

Figure 14: After about 1200 simulated seconds the oscillating swarm transitions into a steady state.

Boid configuration for $\bar{n}$ sine approximation

c_a	c_c	c_s	c_w	c_r	a_{max}	v_{max}	d_{min}
0.76	0.95	0.53	0.36	0.76	12.15	7.16	4.12

Table 3: Evolved swarm parameters that result in the neighborhood function $\bar{n}(t)$ of Figure 13. The corresponding swarms display oscillating behaviors ($\alpha = 2.64$, $l = 7.86$).

Summary and Future Work

Agent states and neighborhood relations are inseparable in swarm systems. Therefore, the dynamics of a swarm can be measured as the fluctuations in perceived neighbors. Based on this approach we are able to characterize the dynamics of boid swarms that exhibit various flocking formations. Hereby, we also identify phases and phase transitions of the boid system, including limit cycles and stead states.

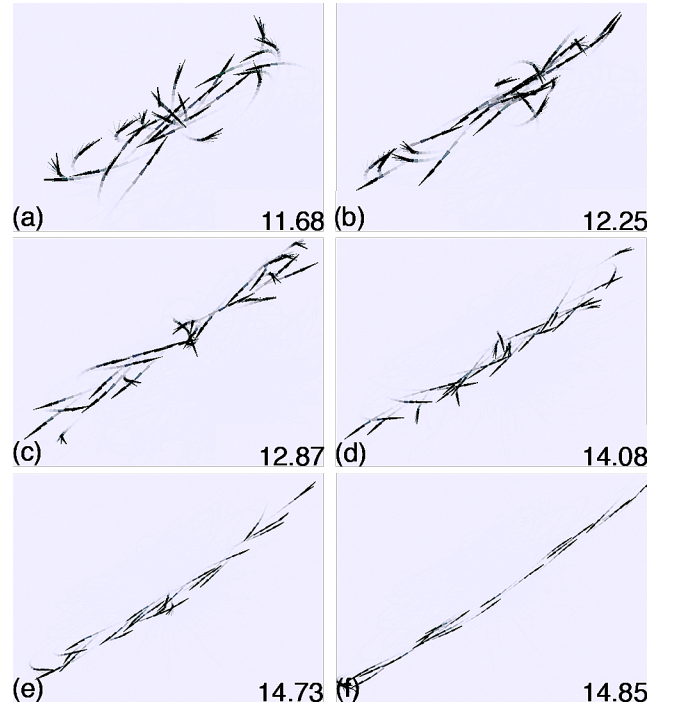Vice-versa, we evolve boid configurations to approximate characteristic neighborhood functions. Here we show that

(a) 11.68 (b) 12.25

(c) 12.87 (d) 14.08

(e) 14.73 (f) 14.85

Figure 15: The flock extends in two directions.

(a) 19.96 (b) 20.90

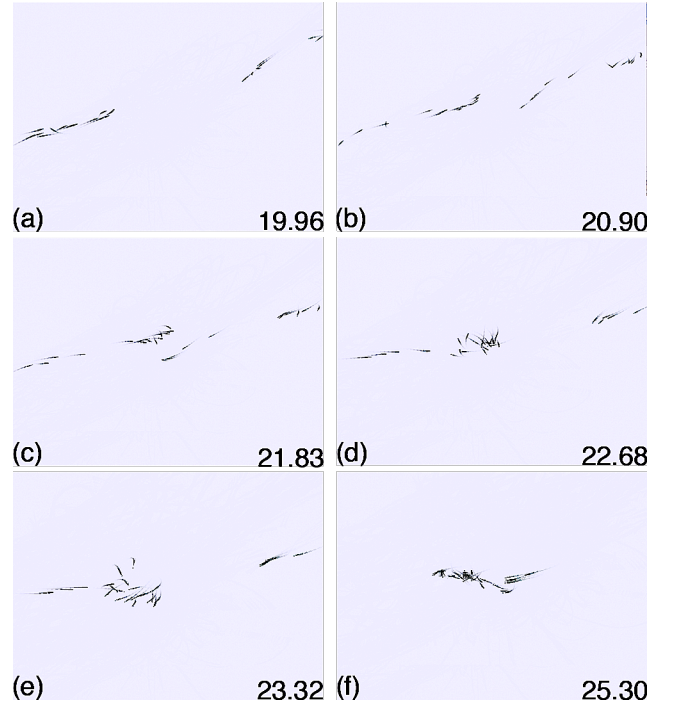(c) 21.83 (d) 22.68

(e) 23.32 (f) 25.30

Figure 16: The previously extended flock from Figure 15 contracts again.

non-linear and oscillating neighborhood developments can emerge in spatially organized homogeneous swarms that
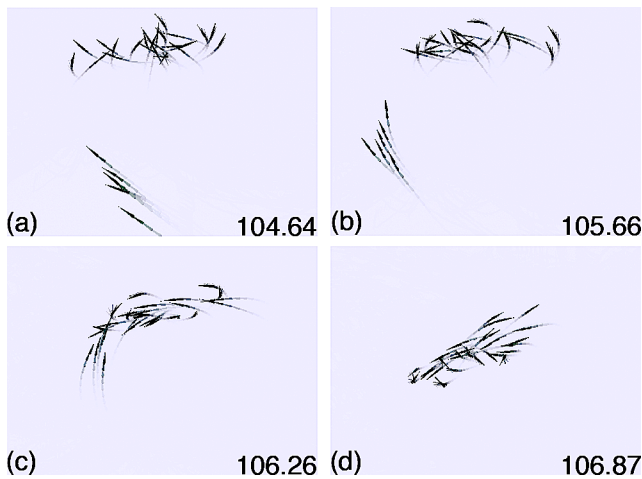
Figure 17: A second flock approaches and joins the other one (continued from Figure 16).
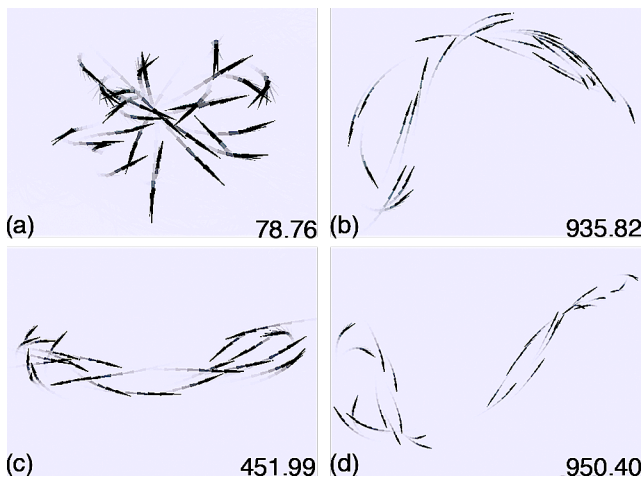

Figure 18: Motion blurring renders some of the more complex flight patterns identifiable: (a) Spherical formation, (b) a U-bent figure-eight, (c) and (d) extended figure-eights.

solely rely on linearly scaled flight acceleration based on repulsion and attraction.

As in studies of complex pattern formations in two dimensional CA (Wolfram (1984)), experimental data suggests that (1) Varying initial conditions and noise influence the evolution of boid flocking patterns locally. The general characteristics of the emerging patterns, however, are mainly based on the flocking parameters of the swarm. (2) Different swarm configurations can lead to very different pattern formations. (3) Chaotic behavior — unexpected, chance-based phase transitions — can occur in systems that initially show orderly, periodic patterns.

For further investigation, we suggest the creation of an abstract swarm model. It has to maintain the link between state and neighborhood, but should be reducible to any high-dimensional space. It would be desirable to find operators that comply with the amalgamation of time and space, or respectively structure and state, without realization of physics. With a generalized set of operators that change states and neighborhood relations concurrently, a systematic classification of swarm dynamics might be possible. Thereby, swarms could become an important model for the dynamics of complex systems in general.

References

Albert, R. (2004). Boolean modeling of genetic regulatory networks. *Complex Networks*, pages 459–481.

Dasgupta, D. (Nov. 2006). Advances in artificial immune systems. *Computational Intelligence Magazine, IEEE*, 1(4):40–49.

del Rey, A., White, S., and Sánchez, G. (2006). A model based on cellular automata to simulate epidemic diseases. *Cellular Automata*, pages 304–310.

Gardner, M. (1970). Mathematical games: The fantastic combinations of john conway's new solitaire game "life". *Scientific American*, 223:120–123.

Hidalgo, C. A. and Barabasi, A.-L. (2006). Scale-free networks. *Scholarpedia: The free peer reviewed encyclopedia*.

Jacob, C. and Burleigh, I. (2004). Biomolecular swarms - an agent-based model of the lactose operon. *Natural Computing: an international journal*, 3(4):361–376.

Kauffman, S. (1995). *At Home in the Universe: The Search for the Laws of Self-Organization and Complexity*. Oxford University Press.

Kwong, H. and Jacob, C. (2003). Evolutionary exploration of dynamic swarm behaviour. In *Congress on Evolutionary Computation*, Canberra, Australia. IEEE Press.

Litman, G. W., Cannon, J. P., and Dishaw, L. J. (2005). Reconstructing immune phylogeny: new perspectives. *Nat Rev Immunol*, 5(11):866–879.

Neelamkavil, F. (1994). *Computer Simulation and Modelling*. John Wiley and Sons.

Oilek, M. and Klein, P. (1979). Stochastic model of the immune response. *Modelling and Optimization of Complex System*, pages 15–25.

Reynolds, C. W. (1987). Flocks, herds, and schools: A distributed behavioral model. In *SIGGRAPH '87 Conference Proceedings*, volume 4, pages 25–34.

Serra, R., Villani, M., and Agostini, L. (2003). On the dynamics of scale-free boolean networks. *Neural Nets*, pages 43–49.

von Neumann, J. and Burks, A. W. (1966). *Theory of self-reproducing automata*. University of Illinois Press, Urbana and London.

Wolfram, S. (1984). Cellular automata as models of complexity. *Nature*, 311:419–424.

Wolfram, S. (2002). *A new kind of science*. Wolfram Media Inc., Champaign, Ilinois, US, United States.